Drag Coefficients of Single Bubbles under Normal and Micro Gravity Conditions*

Akio TOMIYAMA**, Isao KATAOKA***,
Iztok ZUN**** and Tadashi SAKAGUCHI**

Simple but reliable correlations for a drag coefficient, C_D, of single bubbles under a wide range of fluid properties, bubble diameter and acceleration of gravity were developed based on a balance of forces acting on a bubble in a stagnant liquid and available empirical correlations of terminal rising velocities of single bubbles. The proposed C_D consists of three equations, each of which corresponds to pure, slightly contaminated and contaminated systems. The effect of a frictional pressure gradient due to a liquid flow is also taken into account by introducing a concept of an effective body acceleration. Terminal rising velocities of single bubbles were calculated using the proposed C_D, and compared with measured data under the condition of $10^{-2} < Eo < 10^3$, $10^{-14} < M < 10^7$ and $10^{-3} < Re < 10^5$ where Eo, M and Re are Eötvös, Morton and bubble Reynolds numbers, respectively. As a result, it was confirmed that the proposed C_D gives better predictions than available drag coefficient models.

1. Introduction

Reliable models of an interfacial drag force acting on a single bubble in an infinite stagnant liquid are prerequisite for accurate predictions of gas-liquid two-phase bubbly flows. A number of theoretical and experimental studies have been therefore conducted to evaluate a drag coefficient C_D of single bubbles in various stagnant liquids[1]-[9]. As can be found in the well-known book, "Bubbles, Drops, and Particles" written by Clift et al.[1], C_D strongly depends on fluid properties, bubble equivalent diameter, gravity and the degree of contamination on the gas-liquid interface. In addition, Zun and Groselj[2] recently clarified that C_D is related to the characteristics of bubble nonequilibrium movement. In spite of these numerous works, there are few available C_D models which

consider all the effects mentioned above. Although Peebles and Garber[3] and Ishii and Chawla[4] proposed simple C_D models which cover a wide range of fluid properties and bubble diameters, their models were developed only for a contaminated system and therefore they cannot give good predictions for a pure system.

The purpose of this study is to develop a simple and reliable C_D model which takes into account the effects of fluid properties, gravity, bubble diameter and the degree of contamination. In practice, it is not easy to quantitatively evaluate the degree of contamination for a given system. Hence, we will classify the degree of contamination into three groups; pure, slightly contaminated and contaminated systems. In the case of an air-water system, tap water may correspond to the contaminated system, water carefully distilled two or more times belongs to the pure system, and water with a purity level in between to the slightly contaminated system. Although this classification is somewhat ambiguous, C_D correlations based on the three-level classification may be more convenient for practical application than correlations requiring quantitative information on the contamina-

tion. We will develop a C_D model for each system based on a balance of forces acting on a bubble, bubble-size dependent governing factors of terminal rising velocity, and available theoretical and empirical C_D models. In addition, a drag force model for a single bubble in a pipe flow is proposed for the evaluation of a relative velocity between the bubble and liquid under a micro gravity condition.

2. Governing Factors of a Drag Coefficient under a Terminal Condition

Let us derive a fundamental relationship among dimensionless numbers which holds for a single rising bubble in a stagnant liquid under a terminal condition. Grace[5] demonstrated that available measured terminal velocities can be correlated with the following dimensionless numbers:

$$Re = \frac{\rho_L V_T d}{\mu_L} \qquad (1)$$

$$Eo = \frac{g(\rho_L - \rho_G)d^2}{\sigma} \qquad (2)$$

$$M = \frac{g\mu_L^4(\rho_L - \rho_G)}{\rho_L^2 \sigma^3} \qquad (3)$$

where the subscripts G and L denote the gas and liquid phases respectively, ρ the density, V_T the terminal velocity, d the sphere volume equivalent bubble diameter, μ the viscosity, g the acceleration of gravity and σ the surface tension. The bubble Reynolds number Re represents the nondimensional terminal velocity and the ratio of inertia to viscous drag force, the Eötvös number Eo is the ratio of buoyancy to surface tension force and the Morton number M is the property group of the two phases. Grace conducted a dimensional analysis and clarified that Re is a function of Eo and M, i.e., $Re = Re(Eo, M)$. This relationship can also be derived from the balance of drag and buoyancy forces:

$$C_D \frac{1}{2} \rho_L V_T^2 \frac{\pi d^2}{4} = (\rho_L - \rho_G)g \frac{\pi d^3}{6} \qquad (4)$$

where C_D is the drag coefficient. Solving Eq.(4) for V_T^2 yields

$$V_T^2 = \frac{4(\rho_L - \rho_G)gd}{3C_D\rho_L} \qquad (5)$$

Multiplying both sides of the above equation by $(\rho_L d/\mu_L)^2$ gives

$$Re^2 = \frac{4}{3C_D}\sqrt{\frac{Eo^3}{M}} \qquad (6)$$

which indicates $Re = Re(Eo, M)$.

Next, let us consider the governing factors of terminal conditions. It has been clarified by a number of studies that bubbles under terminal conditions can be classified into three types as shown in Fig. 1. Bubbles take spherical shapes when d is small or σ is high. In this case, bubble motions are more or less rectilinear. However their terminal velocities are
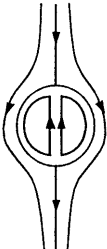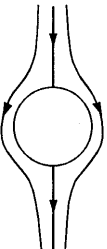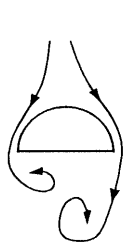

Fig. 1 Governing factors of terminal conditions

Shape	spherical		non-spherical
Motion	rectilinear		fluctuating
Purity	pure	contaminated	both
Flow pattern			
Governing effects	viscosity	viscosity	surface tension and gravity
Relevant dimensionless number	Re	Re	Eo

considerably affected by the degree of contamination on the gas-liquid interface. If the interface is pure, an internal circulation is induced in a bubble, which decreases the viscous drag and increases the terminal velocity. On the contrary, the accumulation of impurities on the bubble interface will occur in the contaminated system, which causes the interface to behave as if it were a rigid surface. This is the reason why the terminal velocity of the contaminated spherical bubble agrees well with that of a rigid spherical particle. The fact that V_T depends on the degree of contamination implies that C_D for spherical bubbles is governed by Re.

On the other hand, bubbles take non-spherical shapes when d is large or σ is low. In this case, the bubble motions are no longer rectilinear and their terminal velocities are little affected by the contamination. This fact implies that the governing factor of the non-spherical bubbles is not the viscous force but the gravity and surface tension forces. It follows that C_D for the non-spherical bubbles should be expressed in terms of Eo.

3. Drag Coefficients of Single Bubbles

A model of C_D is presented in this section based on the classification described above. The validity of the proposed model will be discussed later.

3.1 Spherical bubbles in pure systems

Hadamard[6] presented a theoretical model of C_D for a spherical bubble in a pure system given by

$$C_D = \frac{16}{Re} \qquad (7)$$

which is valid only for low Re, i.e., $Re \le 1$. On the other hand, Levich[7] derived the following C_D for spherical bubbles at high Re:

$$C_D=\frac{48}{Re} \tag{8}$$

which agrees well with the measured data for high Re. Since Eq.(7) has no intersections with Eq.(8), we modified Eq.(7) as

$$C_D=\frac{16}{Re}(1+0.15Re^{0.687}) \tag{9}$$

This modification is based on a standard drag coefficient for a rigid spherical particle given by Eq.(11). Then, Eqs.(8) and (9) have an intersection at $Re=43.4$. The validity of this modification will be discussed later.

Since the value of C_D given by Eq.(9) is greater than that by Eq.(8) for $Re<43.4$, we can summarize the C_D for spherical bubbles in a pure system as:

$$C_D=\min\left[\frac{16}{Re}(1+0.15Re^{0.687}),\frac{48}{Re}\right] \tag{10}$$

3.2 Spherical bubbles in contaminated systems

It has been recognized that the following standard C_D of a rigid spherical particle[8],

$$C_D=\frac{24}{Re}(1+0.15Re^{0.687}) \tag{11}$$

is applicable to spherical bubbles for $Re<1000$ when the interface is contaminated. However, it was confirmed by our comparisons between Eq.(11) and available experimental data that Eq.(11) gives somewhat larger values than the measured C_D when Re is high and the interface is only slightly contaminated. In this case,

$$C_D=\frac{72}{Re} \tag{12}$$

was found to be more appropriate. As a result, we summarized the C_D for spherical bubbles in a slightly contaminated system as:

$$C_D=\min\left[\frac{24}{Re}(1+0.15Re^{0.687}),\frac{72}{Re}\right] \tag{13}$$

On the other hand, when the interface is fully contaminated, we recommend Eq.(11) instead of Eq.(13).

3.3 Non-spherical bubbles

Grace[5] adopted the following correlation for $Eo>40$ and $Re>100$ when he developed a graphical correlation of terminal velocities and shapes of single bubbles:

$$Re=0.70\left(\frac{Eo^3}{M}\right)^{0.25} \tag{14}$$

Substituting Eq.(14) into Eq.(6) yields

$$C_D=\frac{8.16}{3}=2.72 \tag{15}$$

Ishii and Chawla[4] also recommended

$$C_D=\frac{8}{3}=2.67 \tag{16}$$

for $Eo>16$. Equations (15) and (16) indicate that C_D at high Eo and high Re is almost constant.

For $Eo<40$ and $M<10^{-3}$, Grace et al.[9] proposed

the following empirical correlation of Re:

$$Re=\frac{1}{M^{0.149}}\left\{3.42\left[\frac{4}{3}EoM^{-0.149}\left(\frac{\mu_L}{\mu^*}\right)\right]^{-0.14}-0.857\right\} \tag{17}$$

where μ^* is a constant, $0.009\ \mathrm{Ns/m^2}$. Substituting Eq.(17) into Eq.(6) gives

$$C_D=\frac{4}{3}\sqrt{\frac{Eo^3}{M}}\frac{M^{0.298}}{\left\{3.42\left[\frac{4}{3}EoM^{-0.149}\left(\frac{\mu_L}{\mu^*}\right)\right]^{-0.14}-0.857\right\}^2} \tag{18}$$

which is a rather complicated expression for the application to CFD programs.

For non-spherical bubbles under the condition of $Eo<16$, Ishii and Chawla[4] adopted a simple correlation given by

$$C_D=\frac{2}{3}\sqrt{Eo} \tag{19}$$

Equations (16) and (19) are consistent with the experimental evidence that C_D for non-spherical bubbles depends on the gravity and surface tension forces but not on the viscous force. However Eq.(19) gives the terminal velocity

$$V_T=\sqrt{2}\left(\frac{\sigma g(\rho_L-\rho_G)}{\rho_L^2}\right)^{0.25} \tag{20}$$

which does not depend on the bubble diameter so that it cannot account for the effects of the bubble diameter on the terminal rising velocity for $Eo<16$.

Now let us consider another approach to the modeling of C_D for non-spherical bubbles. If the viscous force is negligible, the existence of the bubble can be regarded as a kind of disturbance applied on the gas-liquid interface. If a disturbance is added on a free surface of a stagnant liquid, the disturbance will propagate through the liquid in the form of a gravity and surface tension wave. Similarly, the disturbance caused by the bubble will propagate through the liquid with a phase velocity of the wave. As is well known[10], the phase velocity of the surface tension and gravity wave is given by

$$c^2=\frac{2\pi\sigma}{\rho_L\lambda}+\frac{(\rho_L-\rho_G)g\lambda}{2\pi\rho_L} \tag{21}$$

where λ is the wave length. The first and second terms of the right-hand side of Eq.(21) correspond to the surface tension wave (ripple) and gravity wave (long wave), respectively. The surface tension wave is dominant if λ is small and the gravity wave is dominant if λ is large. As is schematically shown in Fig. 2, when a spherical bubble is rising at a constant velocity V, the liquid velocity over the entire gas-liquid interface is postulated to be V, provided that the interface behaves as a rigid surface. Hence, if we define an azimuthal angle θ as shown in Fig. 2, the velocity component normal to the interface, V_n, is a sinusoidal function of a period 2π. This velocity
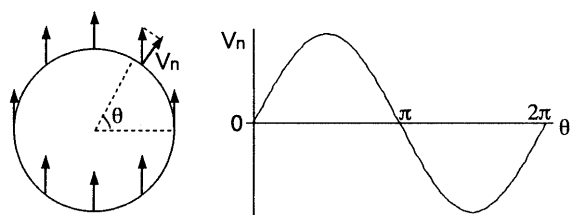
Fig. 2 Liquid velocity distribution on bubble interface

distribution is equivalent to a velocity distribution of a water wave on a free flat surface. As a result, we can regard the bubble as a source of a wave whose principal wavelength is

$$\lambda = \pi d \qquad (22)$$

Even if a bubble is a non-spherical bubble whose shape changes with time, the wave velocity is given by Eq.(21) since there is no source of dispersion in a homogeneous liquid. In addition, the wavelength of the first mode can be approximately estimated using Eq.(22) even for the case of a "fluid interface". Therefore the phase velocity of the wave caused by the bubble is given by

$$c^2 = \frac{2\sigma}{\rho_L d} + \frac{(\rho_L - \rho_G) g d}{2\rho_L} \qquad (23)$$

Next, let us examine the relation between the phase velocity and terminal velocity. If the bubble diameter d is small, the terminal velocity V_T is governed by the viscous force and C_D can be evaluated using either Eq.(10) or Eq.(13). In this case, V_T increases with d. Therefore if d exceeds a certain value, V_T given by Eq.(10) or Eq.(13) becomes larger than the phase velocity c given by Eq.(23). It follows that the velocity of the liquid on the interface, which is a medium of the wave propagation, becomes larger than the phase velocity of the wave. This cannot occur physically. Thus, when the terminal velocity governed by the viscous force exceeds the phase velocity, the terminal velocity must be bounded by the phase velocity c. This might be the reason why the governing force of the terminal velocity quickly changes from the viscous force to the gravity and surface tension forces when the bubble diameter exceeds a certain value.

As a result of the above consideration, we can postulate that when the phase velocity c is less than the viscous force dependent terminal velocity, the terminal velocity for non-spherical bubbles is given by

$$V_T^2 = \frac{2\sigma}{\rho_L d} + \frac{(\rho_L - \rho_G) g d}{2\rho_L} \qquad (24)$$

Although Mendelson[11] proposed a similar model given by

$$V_T^2 = \frac{2\sigma}{\rho_L d} + \frac{g d}{2} \qquad (25)$$

and Marrucci et al.[12] proposed the same correlation

with Eq.(24), no physical interpretation of Eqs.(24) and (25) was made by them so the reasons why the wavelength is given by Eq.(22) and why the governing forces changes at a certain bubble diameter have not been explained. This might be one of the main reasons why Eq.(24) was not adopted in the studies of Grace and Ishii and Chawla.

Although the above-described interpretation of Eq.(24) is also based on the physical intuition and its validity must be theoretically proved in the future, we will adopt Eq.(24) as a basis of C_D for non-spherical bubbles. Multiplying Eq.(24) by $(\rho_L d/\mu_L)^2$ yields

$$Re^2 = \frac{1}{2}\sqrt{\frac{Eo}{M}}(Eo+4) \qquad (26)$$

Substituting Eq.(26) into Eq.(6) gives

$$C_D = \frac{8}{3}\frac{Eo}{Eo+4} \qquad (27)$$

which takes quite a simple form and is expressed in terms of Eo. In addition, Eq.(27) reduces to 8/3 with increasing Eo so that Eq.(27) is consistent with Eqs.(15) and (16) when Eo is high, i.e., when the gravity wave is dominant. On the other hand, when Eo is low and the surface tension wave is dominant, Eq.(27) approximately reduces to

$$C_D = \frac{2}{3}Eo \qquad (28)$$

which yields

$$V_T = \sqrt{2}\left[\frac{\sigma}{\rho_L d}\right]^{1/2} \qquad (29)$$

The above equation is equivalent to the following correlation proposed by Peebles and Garber[3] for "the region 3" of their terminal velocity model:

$$V_T = 1.35\left[\frac{\sigma}{\rho_L d}\right]^{1/2} \qquad (30)$$

Consequently, it was confirmed that Eq.(27) is quantitatively consistent with the available correlations for non-spherical bubbles.

3.4 Summary of the drag coefficient

Under the flow conditions for which we must use the C_D for non-spherical bubbles, the value of C_D for non-spherical bubbles becomes larger than that for spherical bubbles. Hence, all we have to do is to select the larger value of the two drag coefficients. As a result, we can summarize the drag coefficient in a simple form as:

(a) for a pure system (Eqs.(10) and (27))

$$C_D = \max\left\{\min\left[\frac{16}{Re}(1+0.15Re^{0.687}), \frac{48}{Re}\right], \frac{8}{3}\frac{Eo}{Eo+4}\right\} \qquad (31)$$

(b) for a slightly contaminated system (Eqs.(13) and (27))

$$C_D = \max\left\{\min\left[\frac{24}{Re}(1+0.15Re^{0.687}), \frac{72}{Re}\right],$$

$$\left.\frac{8}{3}\frac{Eo}{Eo+4}\right\} \qquad (32)$$

(c) for a fully contaminated system (Eqs. (11) and (27))

$$C_D=\max\left\{\frac{24}{Re}(1+0.15Re^{0.687}),\ \frac{8}{3}\frac{Eo}{Eo+4}\right\} \qquad (33)$$

3.5 Zero and micro gravity conditions

As can be easily understood from Eq. (5), a bubble will not move at all in the absence of gravity. However Kamp, et al.[13] pointed out that if a bubble under a micro or zero gravity condition is in a pipe flow, it will have a finite relative velocity due to a frictional pressure gradient. In order to take into account the effect of the frictional pressure gradient, let us consider a single bubble moving inside a vertical pipe in which liquid is flowing in the vertical direction. According to Clift, et al.[1], the effect of the pipe wall on C_D is negligible if the ratio of the bubble diameter d to the pipe diameter D is less than 0.125. Hence, we assume $d/D<0.125$ and that the bubble is flowing along the center axis of the pipe. In this case, the momentum balance for the fully-developed liquid flow is given by

$$0=-\frac{dP}{dz}-\frac{f}{2D}\rho_L\overline{V_L}^2-\rho_L g \qquad (34)$$

where P is the pressure, z the axial coordinate, f the wall friction factor and $\overline{V_L}$ the mean velocity of the liquid phase. On the other hand, the momentum balance for the bubble is given by

$$0=-\frac{dP}{dz}-\frac{3}{4d}C_D\rho_L V_R^2-\rho_G g \qquad (35)$$

Here V_R is the relative velocity defined by

$$V_R=V_B-V_{L\ max} \qquad (36)$$

where V_B is the bubble velocity and $V_{L\ max}$ the liquid velocity at the center of the pipe.

Eliminating dP/dz from Eqs. (34) and (35) yields

$$\frac{3}{4d}C_D\rho_L V_R^2=(\rho_L-\rho_G)\left[g+\frac{f}{2D}\frac{\rho_L}{\rho_L-\rho_G}\overline{V_L}^2\right] \qquad (37)$$

The above equation implies that the frictional pressure gradient due to the liquid flow is regarded as an additional source of buoyancy. Hence, we introduce a concept of a flow-induced body acceleration g_F and an effective body acceleration g^*, which are defined by

$$g_F=\frac{f}{2D}\frac{\rho_L}{\rho_L-\rho_G}\overline{V_L}^2 \qquad (38)$$

$$g^*=g+g_F \qquad (39)$$

Under the normal gravity condition, g_F is much less than g, so that we can neglect the effect of g_F on g^*. However, if we consider a bubble motion under a micro or zero gravity condition, g_F will play a dominant role in the bubble relative velocity. Using g^*, we can define effective Eötvös and Morton numbers as follows:

$$Eo^*=\frac{g^*(\rho_L-\rho_G)d^2}{\sigma} \qquad (40)$$

$$M^*=\frac{g^*\mu_L^4(\rho_L-\rho_G)}{\rho_L^2\sigma^3} \qquad (41)$$

Replacing Eo in Eqs. (31)-(33) with Eo^*, we can include the effect of the frictional pressure gradient into the drag coefficient model. Then, the relative velocity V_R can be evaluated with the modified C_D and Eq. (37).

4. Verification

The validity of the proposed C_D, Eqs. (31)-(33), was examined through comparisons with measured data and the C_D models proposed by Peebles and Garber[3] and by Ishii and Chawla[4]. We can rewrite their models in terms of Eo and M as:

(d) Peebles and Garber's (PG) model:

$$C_D=\max\left\{\max\left[\frac{24}{Re},\frac{18.7}{Re^{0.68}}\right],\ \min[0.0275M\ Re^4,\right.$$
$$\left. 0.83M^{0.25}Re]\right\} \qquad (42)$$

(e) Ishii and Chawla's (IC) model:

$$C_D=\max\left\{\frac{24}{Re}(1+0.1Re^{0.75}),\ \min\left[\frac{2}{3}\sqrt{Eo},\frac{8}{3}\right]\right\} \qquad (43)$$

The constant, 24, in Eqs. (42) and (43) indicates that the PG and IC models were developed for single bubbles in contaminated systems. Since Eq. (42) includes M and Re for the non-spherical bubble regime, the accuracy of the PG model may not be so good.

Figure 3 shows comparisons of the measured and calculated Re for a wide range of Eo and M, i.e., $10^{-2}<Eo<10^3$ and $10^{-14}<M<10^7$. The measured data denoted by various symbols were quoted from Grace[5]. The solid curves in Figs. 3(a),(b) and (c) were calculated by the PG, IC and present models, respectively. As was expected, the PG model could not give good predictions for non-spherical bubbles at high Eo and low M. On the other hand, the IC model gave good predictions for non-spherical bubbles. However, the IC and PG models failed in predicting Re of spherical bubbles at low Eo and high M except for the three cases, $M=2.6\times10^{-11}(\blacktriangledown)$, $1.6\times10^4(\square)$ and $1.0\times10^7(\bullet)$. It follows that the measured data for these three cases were obtained in contaminated systems and the others were obtained in pure systems, since the PG and IC models were developed for contaminated systems. Hence, Eq. (32), which is for a slightly contaminated system, was applied to these three cases and Eq. (31) was applied to the other cases to examine the validity of the present model. As shown in Fig. 3(c), the present model gave better predictions for all the ranges of Eo and M than the others.

Then, let us examine the validity of the modification from Eq. (7) to Eq. (9). The measured Re

Morton Number						
$+ : 3.6 \times 10^{-14}$	$\times : 9.9 \times 10^{-12}$	$\blacktriangledown : 2.6 \times 10^{-11}$	$\triangle : 4.3 \times 10^{-10}$	$\blacktriangle : 2.4 \times 10^{-9}$	$\blacklozenge : 7.5 \times 10^{-8}$	$\diamondsuit : 8.0 \times 10^{-7}$
$\boxplus : 5.7 \times 10^{-6}$	$\square : 1.6 \times 10^{-4}$	$\blacksquare : 3.5 \times 10^{-4}$	$\circledast : 1.5 \times 10^{-2}$	$\oplus : 0.22$	$\blacklozenge : 3.8$	$\blacksquare : 66$
$\bigcirc : 1.9 \times 10^{2}$	$\triangle : 5.6 \times 10^{2}$	$\triangledown : 4.9 \times 10^{3}$	$\oplus : 1.4 \times 10^{5}$	$\triangledown : 9.5 \times 10^{4}$	$\square : 3.9 \times 10^{6}$	$\bullet : 1.0 \times 10^{7}$

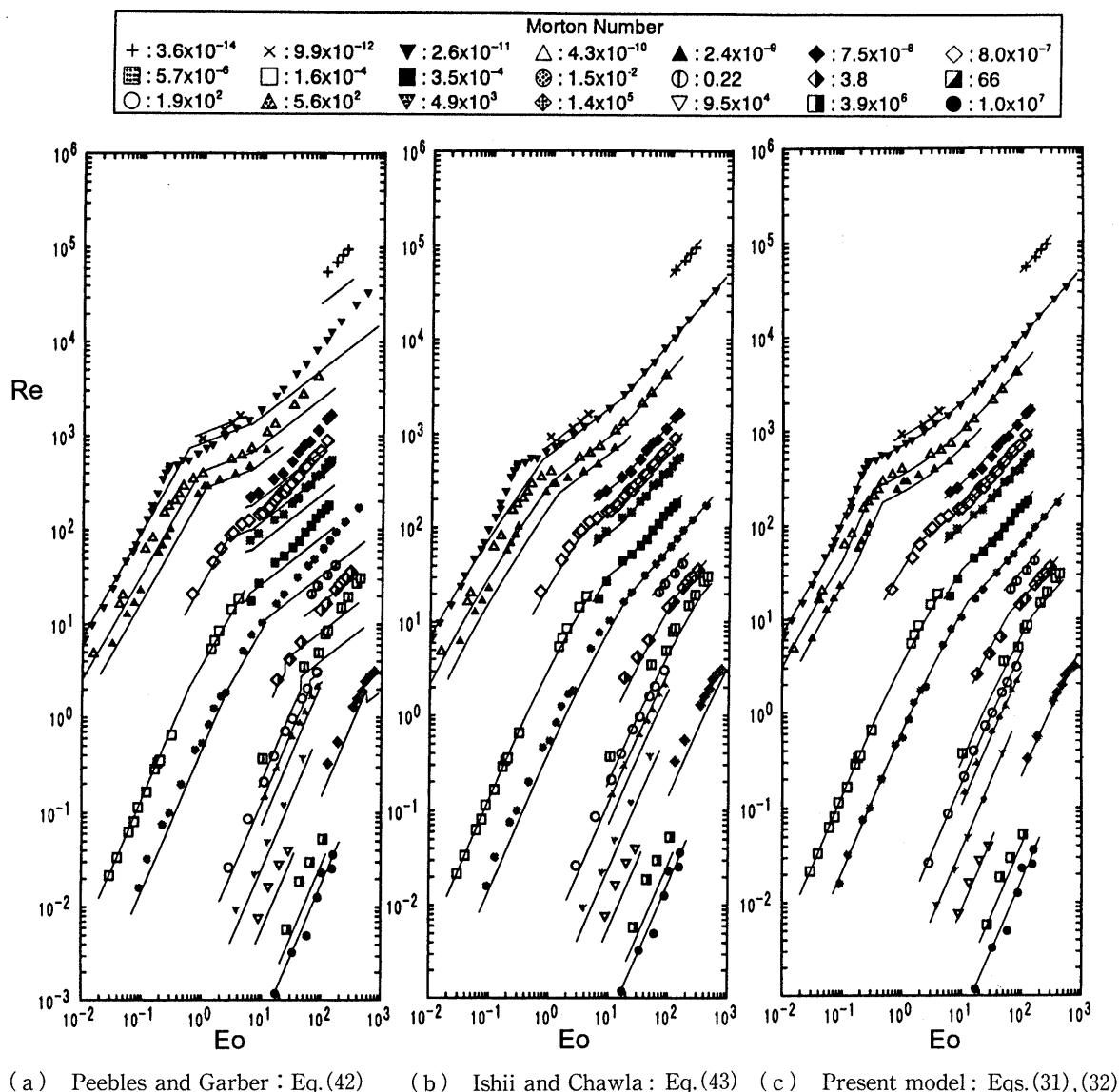(a)　Peebles and Garber ：Eq.(42)　　(b)　Ishii and Chawla：Eq.(43)　(c)　Present model：Eqs.(31),(32)

Fig. 3　Comparisons between measured and calculated Re of single bubbles in various stagnant
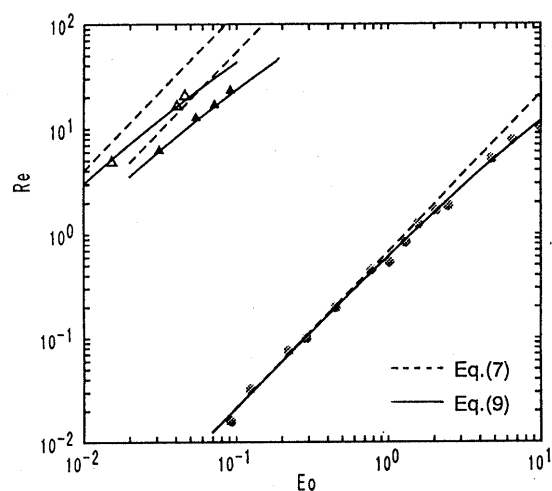liquids; symbols ：measured[5],curves ：calculated

Fig. 4　Verification of Eq.(9) : symbols correspond to
Fig. 3

numbers for spherical bubbles in pure systems were selected from Fig. 3 and compared with Eqs.(7) and (9). As shown in Fig. 4, the modified equation (9) gave better comparisons than Eq.(7).

Figures 5 and 6 show the comparisons between measured and calculated terminal rising velocities of air bubbles in water at atmospheric pressure and room temperature. The measured data were quoted from Clift[1] and the calculation was conducted using the present model (Fig. 5) and IC model(Fig. 6). We can observe a large scattering of the measured data for $0.7 < d < 1.5$ mm, which is due to the difference in the degree of contamination in each measured data. It can be seen from Fig. 5 that(1) C_D for a pure system given by Eq.(31) accurately predicts high terminal velocities appearing in $0.7 < d < 1.5$ mm,(2) C_D for a contaminated system given by Eq.(33) approximately
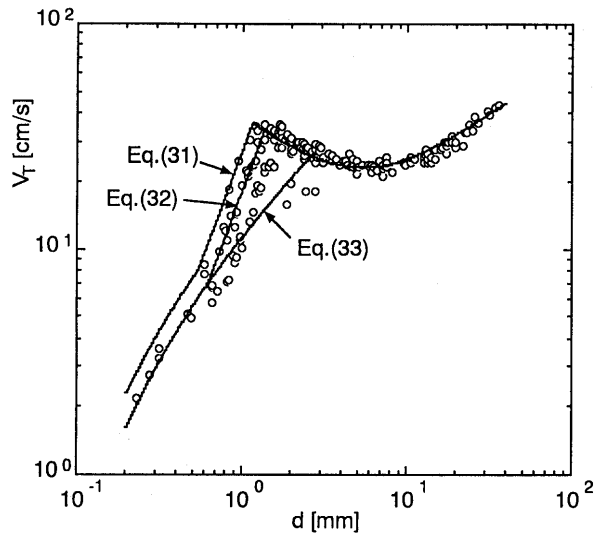
Fig. 5 Comparison between measured and calculated terminal velocities for an air-water system (Present model)
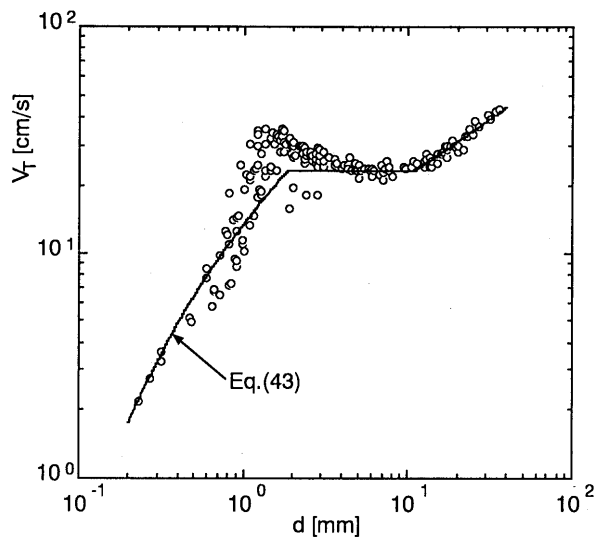

Fig. 6 Comparison between measured and calculated terminal velocities for an air-water system (IC model)

traces the lowest values of the measured V_T, and (3) C_D for a slightly contaminated system given by Eq. (32) agrees with the mean value of the measured V_T. On the other hand, the IC model cannot give good predictions for $0.7 < d < 1.5$ mm since their model was developed only for the contaminated system.

5. Evaluation of Relative Velocity under a Zero Gravity Condition

At present, there is no available information on the magnitude of bubble relative velocity V_R under a zero gravity condition. However Eqs. (31)-(41) enable us to estimate it. If we assume $g=0$, Eq. (37) yields
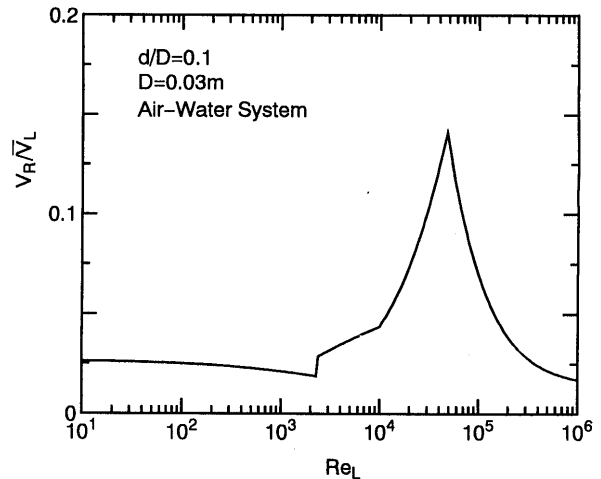

Fig. 7 Relative velocity of a single air bubble in a pipe flow under a zero gravity condition (the bubble is assumed to flow along the pipe axis.)

$$\frac{V_R}{V_L} = \sqrt{\frac{2f}{3C_D}\left(\frac{d}{D}\right)} \qquad (44)$$

For a smooth round tube, the wall friction factor is given by

$$f = \begin{cases} \dfrac{64}{Re_L} & \text{for } Re_L < 2300 \\ \dfrac{0.3164}{Re_L^{0.25}} & \text{for } Re_L \geq 2300 \end{cases} \qquad (45)$$

where Re_L is the liquid Reynolds number defined by

$$Re_L = \frac{\rho_L \overline{V_L} D}{\mu_L} \qquad (46)$$

Figure 7 shows an example of the relationship between Re_L and $V_R/\overline{V_L}$ calculated using Eqs. (44)-(46) and Eq. (31) for an air-water system in a 30 mm I. D. pipe at atmospheric pressure and room temperature. The bubble diameter was assumed as $d = 3$ mm, i.e., $d/D = 0.1$ When the flow is laminar, $V_R/\overline{V_L}$ is less than 2.5% so that we can neglect the relative velocity. On the other hand, the bubble relative velocity increases steeply for $10000 < Re_L < 50000$ due to a large frictional pressure drop of turbulent flow. Then, $V_R/\overline{V_L}$ decreases for $Re_L > 50000$. This is because the relative velocity governed by the viscous drag exceeds the wave velocity. This result indicates that there could be a finite range of Re_L in which we cannot neglect the bubble relative velocity even under a zero gravity condition.

6. Conclusion

A simple but accurate drag coefficient model for single bubbles was developed by making use of a balance of forces acting on a bubble and available theoretical and empirical correlations of terminal rising velocity. The proposed model covers a wide range of fluid properties, gravity and bubble diameter,

and consists of three correlations, each of which corresponds to pure, slightly contaminated, and contaminated gas-liquid systems as follows:

for a pure system

$$C_D = \max\left\{\min\left[\frac{16}{Re}(1+0.15Re^{0.687}), \frac{48}{Re}\right], \frac{8}{3}\frac{Eo}{Eo+4}\right\}$$

for a slightly contaminated system

$$C_D = \max\left\{\min\left[\frac{24}{Re}(1+0.15Re^{0.687}), \frac{72}{Re}\right], \frac{8}{3}\frac{Eo}{Eo+4}\right\}$$

for a contaminated system

$$C_D = \max\left\{\frac{24}{Re}(1+0.15Re^{0.687}), \frac{8}{3}\frac{Eo}{Eo+4}\right\}$$

where C_D is the drag coefficient, Re the bubble Reynolds number and Eo the Eötvös number. Then, the effect of a frictional pressure gradient due to a liquid flow was taken into account by introducing a concept of an effective body acceleration in order to apply the model to zero and micro gravity conditions.

Terminal rising velocities of single bubbles in stagnant liquids were calculated using the proposed model, and compared with measured data under the condition of $10^{-2} < Eo < 10^3$, $10^{-14} < M < 10^7$ and $10^{-3} < Re < 10^5$ where M is the Morton number. As a result, it was confirmed that the proposed C_D gives better predictions for all the ranges of Eo, M and Re than available drag coefficient models. Then, the relative velocity between the bubble and liquid phase in a pipe flow under a zero gravity condition was evaluated using the drag model based on the effective body acceleration, which indicated that there exists a finite range of the liquid Reynolds number for which we cannot neglect the relative velocity even under the zero gravity condition.

References

(1) Clift, R., Grace, J.R. and Weber, M.E., Bubbles, Drops, and Particles, Academic Press, (1978).

(2) Zun, I. and Groselj, J., The Structure of Bubble Non-Equilibrium Movement in Free-Rise and Agitated-Rise Conditions, Nuclear Eng. Des., 163(1996), p. 99.

(3) Peebles, F.N. and Garber, H.J., Studies on the Motion of Gas Bubbles in Liquids, Chem. Eng. Prog., 49, 2(1953), p. 88.

(4) Ishii, M. and Chawla, T.C., Local Drag Laws in Dispersed Two-Phase Flow, ANL-79-105(1979).

(5) Grace, J.R., Shapes and Velocities of Bubbles Rising in Infinite Liquids, Trans. Inst. Chem. Eng., 51(1973), p. 116.

(6) Hadamard, J.S., Mouvement Permanent Lent d'une Sphere Liquide et Visqueuse dans un Liquide Visqueux, C. R. Acad. Sci., 152(1911), p. 1735.

(7) Levich, V.G., Physicochemical Hydrodynamics, Prentice-Hall, New York, (1962).

(8) Clift, R. and Gauvin, W.H., The Motion of Particles in Turbulent Gas Streams, Proc. Chemeca '70, 1(1970), p. 14.

(9) Grace, J.R., Wairegi, T. and Nguyen, T.H., Shapes and Velocities of Single Drops and Bubbles Moving Freely through Immiscible Liquids, Trans. Inst. Chem. Eng., 54(1976), p. 167.

(10) Lamb, H., Hydrodynamics, Cambridge University Press (1932).

(11) Mendelson, H.D., The Prediction of Bubble Terminal Velocities from Wave Theory, A. I. Ch. E. J., 13, 2(1967), p. 250.

(12) Marrucci, G., Apuzzo, G. and Astarita, G.A., Motion of Liquid Drops in Non-Newtonian Systems, A. I. Ch. E. J., 16, 4(1970), p. 538.

(13) Kamp, A., Colin, C. and Fabre, J., Bubbly Flow in a Pipe: Influence of Gravity upon Void and Velocity Distribution, Proc. Experimental Heat Transf. Fluid Mech. and Thermodynamics, Vol. 2(1993), p. 1418.